Correlation Analyses between Downward Longwave Radiation Particulate Matters, Aerosol Optical Depth, and Metrological Variables Under Non-Dusty and Cloudless Conditions

abdullrahman maghrabi (amaghrabi@kacst.edu.sa)
King Abdulaziz City for Science And Technology https://orcid.org/0000-0001-5067-057X
Badr Alharbi
King Abdulaziz City for Science and Technology
Hamoud Alharbi
King Abdulaziz City for Science and Technology
Abdulah Aldosari
King Abdulaziz City for Science and Technology

Research Article

Keywords: arid conditions, clear sky, downward long wave, particulate matters, aerosols, meteorological variables.

Posted Date: October 21st, 2021

DOI: https://doi.org/10.21203/rs.3.rs-899650/v1

Version of Record: A version of this preprint was published at Theoretical and Applied Climatology on March 19th, 2022. See the published version at https://doi.org/10.1007/s00704-022-04004-9.

Abstract

This study used downward (LW) radiation measurements, air temperature (T), particulate matter (PM) concentrations of fine ($PM_{2.5}$) and coarse (PM_{10}) particles, aerosol optical depth (AOD), wind speed, and precipitable water vapor (PWV) data from Riyadh, an arid site in central Saudi Arabia, between 2014–2019 to characterize their variations and investigate the influence of these variables on the measured downward LW radiation under non-dusty, clear sky conditions. The LW radiation and air temperature, it was found, attain their maximum in summer and minimum in winter. Conversely, the PM mean concentrations and AOD showed their maximum in spring and minimum in winter. PWV features an increasing trend during spring, summer, and fall, whereas it features a decreasing trend during the winter. The monthly variation of WS shows low monthly values during fall and winter and considerably higher monthly mean variation during spring and summer. Apart from wind speed, which doesn't affect the LW radiation, correlation analyses demonstrated that the LW correlates positively with the remainder of the considered variables. The strength and degree of association between the LW radiation and these variables differ from one variable to another, with air temperature having the strongest correlation (correlation coefficient = 0.98) with the LW radiation, followed by the AOD (correlation coefficient = 0.69), with a correlation coefficient of 0.36 with the PWV. Similarly, the relationships between the LW radiation and both PM_{10} and $PM_{2.5}$ had the same correlation coefficient of 0.32.

The effect of the meteorological variables (mainly air temperature, relative humidity, and wind speed) on the PM concentrations were investigated using the regression analyses. The results showed a significant positive relationship with air temperature and wind speed and a negative relationship with RH.

1. Introduction

Downward long wave (LW) radiation (wavelength 4.0–100 μm) is an important parameter for many applications, such as solar energy, energy budget studies, atmospheric radiation transfer, weather forecasting, and meteorological and environmental applications (e.g., Chou and Ridgway, 1990; Svendsen et al., 1993; Wild et al., 2001; Garcia 2004; Maghrabi and Clay, 2011).

This radiation results from the absorption and re-emission of the infrared (IR) radiation emitted from the Earth's surface due to the presence of greenhouse gases in the atmosphere. This absorption/emission in the atmosphere is caused primarily by water vapor (below 7.6 μm, between 13 μm and 16 μm, and beyond 22 μm), carbon dioxide (from 14 μm to 16 μm) and, to a lesser extent, ozone (between 9 and 10 μm). Trace gases, such as methane, nitrous oxides, and carbon monoxide, also absorb and emit in the IR wavelengths. The remaining unabsorbed portion of the Earth's radiation escapes into outer space through the atmospheric window, which lies between 8 μm and 14 μm (e.g., Idso and Jackson, 1969; Ruckstuhl et al., 2007; Maghrabi 2012; Viudez-Mora et al., 2009) .

Under clear sky conditions, the atmospheric radiation is mainly affected by the atmospheric water content and/or the screen temperatures (Swinbank, 1963; Brutsaert, 1975, Berdahl and Fromberg, 1982;

Prata, 1996; Dilley and O´Brien 1998; Dupont, et al., 2008). However, other factors, such as atmospheric aerosol particles, are expected to affect atmospheric radiation differently (Haywood and Boucher, 2000; Dufresne et al., 2002; Maghrabi et al., 2011; Maghrabi 2012; Maghrabi and Al-Dosari, 2016)

Atmospheric aerosols directly influence the radiation balance through the absorption and scattering of both solar and atmospheric radiation. Moreover, aerosol particles affect cloud formations and distributions, which affect, indirectly, the energy budget and, thereby, the climate. The aerosol effects vary in importance according to several factors, such as wavelength, concentrations, and atmospheric conditions (Liu and Ou, 1990; Smirnov et al., 2002; Xia et al., 2007).

Atmospheric aerosols, termed particulate matter (PM), consist of solid particles, liquid droplets, or mixed-phase particles varying in size from tens of Angstroms to hundreds of microns. PM includes both the coarse PM_{10} (diameter of 2.5 μm to 10 μm) and the fine $PM_{2.5}$ (diameter less than 2.5 μm). The sources of PM_{10} and $PM_{2.5}$ can be natural, such as windborne dust or anthropogenic, such as the combustion of fuels (Harrison, et al., 2004; Barkan et al., 2004; Hueglin, et al., 2005; Alharbi, 2009; Begum, et al., 2011; Chantara, et al., 2012; Chen, et al., 2018).

Despite the importance of atmospheric aerosols/PM and their impact on solar and LW atmospheric radiation, there has been less work conducted in this part of the world to study their effect on LW atmospheric radiation. In light of this, this paper aims to characterize LW radiation's variations, screen level temperature, precipitable water vapor (PWV), wind speed, atmospheric aerosol (PM_{10}, $PM_{2.5}$) concentrations, and atmospheric aerosol optical depth and investigate their relative impact on the cloudless LW radiation in Riyadh.

2. Data Sources And Methodology

Riyadh, Saudi Arabia's capital, owing to fast urbanization and industrialization, is one of the country's most polluted cities. It has more than 7 million inhabitants with great heating, industrial, and traffic activities within cities in Saudi Arabia. These factors, among others, result in a high number of particulate matters of different sizes in Riyadh. Since Riyadh is located in the middle of the Arabian Peninsula and surrounded to the east and west by the two corridors of the Ad-Dahna sand belt and many regional dust sources, dust storms, in addition to local sources, can be considered a major natural source of atmospheric aerosols (Alharbi 2009).

The dataset used here consists of downward longwave (LW) atmospheric radiation measurements, particulate matter concentrations (PM_{10}, $PM_{2.5}$), meteorological data and aerosol optical depth data. Apart from aerosol optical depth data, all the measurements were taken using a radiometric and weather station installed on January 2014 on the rooftop of the radiation detector laboratory building at the King Abdulaziz City for Science and Technology (KACST) campus (Riyadh, central Saudi Arabia; lat. 24 43; long. 46 40; alt. 613 m). The data covered the period from 1 March 2014 to 30 September 2019.

The LW radiation data were measured using a Kipp & Zonen pyrgeometer model CGR3 (CG3 handbook Kipp & Zonen, 2015). It has a 150° field of view and records broadband infrared flux in the wavelength range of 4–50 μm. The specifications of this detector and its calibration processes can be found on the Kipp & Zonen website.

Meteorological data such as atmospheric pressure, relative humidity, wind speed and directions, and air temperature were measured using the Skye Mini Metstation (Skye instrument, 2015) that incorporates different meteorological sensors. Dataloggers CR23X and CR10X were programmed at 30- and 10-s sampling rates respectively, and both provided measurements at every 10- and 60-min integration time.

The total integrated water content, namely the PWV, was calculated using the model developed by Maghrabi and Al dajani (2013). As per this model, the PWV values were calculated from the measurements of the vapor pressure and air temperature. PWV is the amount of liquid water that would be obtained if the entire vapor in the atmosphere within the vertical column was compressed to the point of condensation.

The concentrations of PM_{10} and $PM_{2.5}$ were measured using beta attenuation monitors (BAM 1020, Met One Instruments) based on the principle of the beta ray attenuation method. In this study, two monitors were used, with each one featuring a size-selective inlet, a beta radiation source and detector, and a filter tape. PM_{10} and $PM_{2.5}$ were sampled through the respective size-selective inlet installed in each monitor and deposited on a single point on a filter tape. The mass of deposited PM_{10} and $PM_{2.5}$ were determined by calculating the difference between the beta radiation transmitted through the filter tape before and after taking the PM_{10} and $PM_{2.5}$ samples.

The aerosol optical Depth at 500 nm (AOD_{500}) data between 1 March 2014 to August 2015 from the AERONET solar village site located 15 km North-West of KACST were used. The hourly averaged Level 1.5 products were utilized, which were cloud-screened and quality assured (Holben et al., 2001). The instrumentation, data acquisition, retrieval algorithms and calibration procedure for the used instruments are described in detail in several studies (e.g., Holben et al., 2001; Maghrabi and Alotaib, 2011).

Due to some technical issues, there was a lack of observation data during the study period. However, the observation data covered all the expected atmospheric and environmental conditions experienced in Riyadh.

The clear sky times were selected based on the cloud information provided by the Saudi Presidency of the Environment (SPE). The cloud coverage was required to be less than two octa during the course of measurements. Dusty periods were excluded using the synoptic information provided by the Saudi Presidency of the Environment (SPE). Additionally, dusty periods were excluded using the procedures developed by Alharbi (2003).

Using the above-mentioned quality control procedures, a total of 16022 hours of clear sky measurements during the study period were selected, and their basic statistical values are presented in Table (1).

Table (1) presents the mean, standard deviation, and the minimum and maximum values of the hourly mean values of the variables considered between March 2015 and September 2019. The aerosol optical depth data were recorded between March 2014 to August 2015.

The LW atmospheric radiation ranges between 238.55 and 505.29 Wm^2 with a mean of 383.99 ± 69.75 Wm^2 and a median of 389.9 Wm^2. The PM_{10} ranges between 8 and 442 $\mu g/m^3$ with a mean value of 141.67 ± 71.9 $\mu g/m^3$ and median of 129 $\mu g/m^3$. $PM_{2.5}$ on the other hand has a mean of 39.9 ± 29.3 $\mu g/m^3$, median of 34 $\mu g/m^3$, maximum of 98.51 $\mu g/m^3$, and minimum of 1 µg/m3. The perceptible water vapor and air temperature range between 6.35 and 38.50 mm and 3.41 and 46.22°C respectively with mean values of 19.02 ± 4.35% for the former and 29.21 ± 9.34°C for the latter. The wind speed reaches a maximum of 5.49 m/s and has a minimum of zero and a mean of 1.89 ± 1.50 m/s.

3. Results

3.1 Characterization of the considered variables

Figure (1) shows the monthly variations of the (a) LW radiation, (b) PM_{10}, (c) $PM_{2.5}$, (d) AOD, (e) air temperature (f) PWV, and (g) the wind speed during the study period.

The monthly variations in the LW radiation, PM_{10}, $PM_{2.5}$, air temperature, PWV, and wind speed were 26%, 38 %, 44 %, 59%, 33%, and 40 % respectively. LW radiation displays a minimum in February (317 W/m^2); between February and March, it increases by about 32 Wm^2 and then increases gradually until it reaches a maximum (about 430 W/m^2) in July.

The PM mean concentrations showed their maximum in the spring season and minimum in winter. The PM_{10} and $PM_{2.5}$concentrations increase dramatically from 110 to 166 $\mu g/m^3$ for the former, and from 29 to 43 $\mu g/m^3$ for the latter between February and March. The PM_{10} remains around this value until May and it dropped to 140 $\mu g/m^3$ in June. Between June and July, the PM_{10} jumped from 140 to 180 $\mu g/m^3$ and dropped to 140 $\mu g/m^3$ in August and remained between 140 and 135 $\mu g/m^3$ between August and October and decreased to 110 $\mu g/m^3$ by November. Then, it reached 140 $\mu g/m^3$ by December and decreased to its minimum in February. From its maximum, $PM_{2.5}$ decreased gradually in March to reach its minimum of 30 $\mu g/m^3$ in November. This period is characterized by a dramatic drop of about 16% between July and August and by 21% between October and November with no major changes observed between August and October.

The monthly variation of the atmospheric column of atmospheric aerosols, represented by aerosol optical depth (AOD), is indicated in Figure (1.d), which shows that AOD during the March-August period (spring and summer) features a considerably higher monthly mean variation than during the September–February period (fall and winter). It increases from its lowest mean value in January (0.11) until they reach its maximum in April (0.7). Between March and April (pre-monsoon season), the AOD value rises

due to the high aerosol loads brought to the region by dust storms from local, regional, and global sources (Kutiel and Furman 2003; Alharbi et al., 2013). Subsequently, the AOD value decreases to 0.38 in July. In August, the AOD reaches a value of 0.5 and then decreases steadily till January. The August increase may be due to the high temperature during this month and its influence on the boundary layer which, in consequence, affects the aerosol loads from anthropogenic sources (e.g., Gröbner et al., 2009; Maghrabi and Alotaibi 2017).

The air temperature (Fig. 1.e) increases gradually from its minimum value of 16°C in February to reach its maximum of 39°C in July. Between June and August, the monthly temperature varies by about 1.5°C. The temperature decreases gradually subsequently to attain its minimum.

Figure (1.f) shows that the monthly mean variation of the estimated PWV features an increasing trend during spring, summer, and fall, whereas the variation features a decreasing trend during winter. The increasing trends during spring and summer are comparable. The monthly mean variation of the estimated PWV decreased to its lowest value of ∼14.3 mm in February and increased to its highest value of ∼22 mm in November.

The monthly pattern of the WS curve (Fig. 1.g) features low monthly mean variation during fall and winter and a much higher monthly mean variation during spring and summer. The mean near-surface wind speed decreased to its lowest value of ∼1.5 m/s in October and increased to its peak value of ∼2.7 m/s in July.

3.2 Correlation analyses between LW and the considered variables

Regression analyses between the downward LW radiation and independent variables (meteorological variables, PM_{10}, $PM_{2.5}$, and AOD) were performed and established. The significance of the proposed regressions was tested using F-tests and t-statistic student test. The results have been presented in Table (2).

3.2.1 LW radiation and metrological variables

Figure (2) shows the relationship between the daily mean values of the LW radiation and the considered meteorological variables. The magnitude and the strength of the correlations were different from one variable to another.

The relationship between LW radiation and air temperature (Fig. 2.a) is much clearer, stronger, and extended over the wider ranges of temperature values. The data are less scattered and confined within no more than 1.5 standard deviation. The correlation coefficient, standard deviation, and the slope of the regression between T and LW were 0.98, 27.61 Wm^2, and 6.85 Wm^2/C respectively.

While there is a spread in the data, the LW radiation increases as the total atmospheric water content (PWV) increases. This relationship has a correlation coefficient of 0.36 and a standard deviation of about 37.7 Wm^2. The LW increases by about 5.10 Wm^2 per 1 mm increase in the PWV. The regression analyses between the wind speed and LW radiation showed no significant correlation between the two variables.

3.2.2 LW radiation and PM concentrations

Figure (3) indicates the relationships between the daily mean values of the LW radiation and (a) PM_{10} and (b) $PM_{2.5}$ concentrations..

The scatter in the data of both PM_{10} and $PM_{2.5}$ showed a positive correlation with the LW radiation. The PMs that exist in the atmosphere are capable of absorbing and re-emitting the LW radiation; hence, the LW radiation increases as the PM concentrations increase. The mechanism of longwave absorption and emission by aerosols in different conditions has been described by Dufresne et al (2002).

There are obvious spreads in the data; for e.g., for a certain value of PM values, there are several measurements of different values of the LW radiation. The PM concentration could be increased and affected by different factors, including traffic activities, population intensity, and topography. The long-range transportation of atmospheric aerosols may be another factor that affects the region. The effect of other atmospheric, environmental, and meteorological factors on the LW radiation may contribute to the spread in this relationship. Moreover, the PM concentrations represent the particulate matters with sizes below or equal to the 10 microns measured at ~ 30 m above ground, whereas the atmospheric AOD is integrated for the whole atmospheric column, which is more suitable to represent the total atmospheric extinction.

The LW when correlated with the PM_{10} has a correlation coefficient of 0.32, a standard deviation of 39.29 Wm^2, and a slope of 53.05 Wm^2 per 1 increase in 1 $\mu g/m^3$. It increased by 0.55.79 Wm^2 per 1 $\mu g/m^3$ of $PM_{2.5}$ with a correlation coefficient of 0.32 and a standard deviation of 38.42 Wm^2.

3.2.3 LW radiation and atmospheric AOD

Atmospheric AOD is more suitable to represent the total atmospheric extinction since it is integrated for the whole atmospheric column rather than being a representation at a low level near the ground. Figures (4) is a scatter plot that illustrates the relationship between LW radiation and AOD. Although there is some scatter in the data, the AOD is obviously correlated better with the LW radiation when compared to the PM concentrations.

According to the regression analyses, the LW radiation increased significantly by about 46.26 Wm^2 per 1 increase in AOD. This relationship has a correlation coefficient of 0.69 and a standard deviation of 34.73 Wm^2.

3.2.4 Discussions

The positive relationship between air temperature and LW radiation found in this study is comparable with previous research. The positive correlation between these two variables indicates that the infrared emission in the part of the atmosphere where the radiation originates is correlated via some combination of radiation, turbulence and advective process with the surface temperature (e.g. Maghrabi 2012)

Similarly, the dependence of the LW atmospheric radiation on the PWV arises from the strong absorption and reemission of the infrared radiation in the atmospheric window (8–14 micron), vibro-rotational, and rotational absorption bands of water molecules. However, the strength of the relationship between the LW radiation and the PWV is not stronger than expected. This may be attributed to several causes. These include the use of the empirical model to calculate the PWV, where this model may have its own uncertainties. In practice, the PWV values measured with the radiosondes or GPS receivers are most useful (e.g., Bevis, et al., 1992; Maghrabi and Clay 2010). However, such data are usually not available. Moreover, the effect of other atmospheric conditions may also contribute to the spread in the relationship between LW radiation and PWV.

Interesting results were found by studying the effect of the atmospheric aerosols on LW radiation. Such correlations between the LW radiation and, particularly, PM concentrations are rarely available in the literature, and this work is the first to present such an investigation. The LW radiation was found to increase with an increase in the atmospheric aerosols represented by PM_{10}, $PM_{2.5}$, and AOD. The relationship between the atmospheric aerosols and the downward atmospheric radiation is due to the absorption and reemission of the LW radiation (atmospheric warming) emitted by the aerosol particles, which increases with an increase in aerosol loading (e.g., Dufresne et al., 2002). The absorption of the LW radiation by atmospheric aerosols and the resultant increase in the LW radiation is an important factor to be considered particularly in energy budget studies and climate change modeling. The LW radiation showed stronger dependence on the AOD than the PM concentrations, which is partially because the AOD accounts for all the air/particles found in the atmospheric column, whereas the PM concentrations represent the atmospheric aerosols only at the screen level. The dependence of the LW radiation on the fine ($PM_{2.5}$) and coarse particles (PM_{10}) have the same statistical indicators. The spread in the relationship between the PM concentrations and the LW radiation may be attributed to several factors. These include the prevailing atmospheric and environmental conditions(Easter, et al., 1994; Querol, et al., 2001; Vardoulakis and Kassomenos, 2008; Streets et al., 2009; Akyüz and Cabuk, 2009; Tian, et al., 2012; Dominick, et al., 2012; Jayamurugan, et al., 2013; Wang and Ogawa, 2015; Klingmüller, et al., 2016 Li, et al., 2017; Phairuang, et al., 2017; Fernandes, et al., 2017. For example, the source and sinks of trace gases and aerosol particles in the atmosphere are, indirectly, affected by the variations of air temperature and the water vapor and wind speed at the screen level.

To study this hypothesis, regression analyses between the air temperature, relative humidity, and wind speed and the PM concentrations were conducted as presented in Figure (5). The correlation results showed that the PM concentrations (PM_{10} and $PM_{2.5}$) correlated significantly with the air temperature and wind speed and negatively with the RH. The increase in the air temperature can promote the evaporation of aerosols, whereas an increase in the RH increases the rate of absorption of particulates in

the atmosphere. It is also expected that the AOD may be affected by metrological variations but, based on the obtained results; these effects may be small when compared to PM concentrations. Studying the influence of metrological variables and the PM requires detailed investigations beyond the scope of this study, and it is the subject of an ongoing research project. Although limited studies have been conducted to determine the interactions between meteorological factors and air pollutants in an arid environment, one that is characterized by extreme heat during sunshine and an abrupt drop in temperature at night, extremely low rainfall and extremely high evapotranspiration rates, the obtained results are consistent with those previously conducted and established associations between meteorological conditions and the parameters of air pollutants and quality (Alharbi 2009).

Conclusion

In this study, downward and long wave (LW) radiation measurements, air temperature, particulate matter (PM) concentrations of fine and coarse aerosols, and the aerosol optical depth at 500 nm and the precipitable water vapor from Riyadh, an arid site in central Saudi Arabia, were used to characterize their variations and investigate the influence of these variables on the measured LW radiation. The study reached the following conclusions:

1. LW radiation follows the trend in temperature, which reaches a maximum in summer and a minimum in winter.
2. The monthly variations in the LW radiation, PM_{10}, $PM_{2.5}$, air temperature, PWV, and wind speed were 26%, 38 %, 44, 59%, 33%, and 40 % respectively.
3. The screen temperature shows a better correlation with LW radiation with a correlations coefficient and an RMSE of 0.98 and 8.09 Wm^{-2} respectively.
4. Although water vapor is considered one of the most important greenhouse gases, the correlation between LW and PWV found in this study was reasonable. This may be due to the empirical nature of calculating the PWV. However, the physical relationship between PWV and LW radiation is evident.
5. The PM mean concentrations and AOD showed their maximum in spring and minimum in winter.
6. The relationship between the atmospheric aerosols and the downward atmospheric radiation showed that the LW radiation increases with increased aerosol loading. This is due to the absorption and reemission due to atmospheric aerosols.
7. The effect of the atmospheric aerosols on the LW radiation occurs mainly in the atmospheric window and is controlled by several factors such as the wavelength, weather, and atmospheric conditions.
8. The regression analyses between LW radiation and AOD showed strong positive correlations between the two variables in comparisons with the PM concentration in Riyadh under cloudless and non-dusty conditions.
9. The correlations coefficient between AOD and LW radiation was 0.69; whereas, it was 0.32 when the LW radiation was correlated with PM concentrations.

10. The strong relation between AOD and LW is, partially, due to the fact the AOD represents the total atmospheric extinction integrated for the whole atmospheric column rather than being a representation at a low level near the ground. Moreover, the PM concentrations are more affected by atmospheric and environmental conditions at the screen level.
11. The correlation analyses between the PM concentrations (PM_{10} and $PM_{2.5}$) showed a significant positive relationship with the air temperature and wind speed but a negative relationship with RH.

Declarations

Availability of data and materials

All the data generated from this study are available from the corresponding author upon request.

Funding

Not applicable.

Author contributions

All authors contributed to the study conception and design. Material preparation, data collection, and analysis were performed by Abdullrahman Maghrabi; Badr Alharbi; Hamoud Alharbi; and Abdulah Aldosari. The first draft of the manuscript was written by Abdullrahman Maghrabi, and all authors discussed the results and commented on the manuscript. All authors edited the manuscript and contributed to insightful discussions.

Competing interests

The authors declare no competing interests.

Code availability

No code was used in this study the analyses were carried out using the commercial software.

Ethics approval Not applicable.

Consent to participate Not applicable.

Consent for publication Not applicable.

Conflict of interest The authors declare no competing interests.

Acknowledgements

We would like to thank King Abdulaziz City for Science and Technology (KACST) for supporting this work.

References

1. Akyüz , M., Cabuk, H., 2009. Meteorological variations of PM2.5/PM10 concentrations and particle-associated polycyclic aromatic hydrocarbons in the atmospheric environment of Zonguldak, Turkey. Journal of Hazardous Materials. 170: 13-21.
2. Alharbi, B., Maghrabi, A., Tapper, N., 2013. The March 2009 dust event in Saudi Arabia: precursor and supportive environment. Bull. Amer. Meteorol., 94, 4: 516-527
3. Alharbi, B., 2003. Transport of North African dust to Big Bend, Texas, during the 1999 Big Bend Regional Aerosol and Visibility Observational Study. Masters Thesis, Colorado State University, Colorado.
4. Alharbi, B., 2009: Airborne dust in Saudi Arabia: Source areas, entrainment, simulation and composition. Ph.D. dissertation, Monash University, 313 pp.
5. Barkan, J., Kutiel, H., Alpert, P. 2004. Climatology of Dust Sources in North Africa and the Arabian Peninsula, Based on TOMS Data. Indoor and Built Environment 13:407-419.
6. Begum, B., Biswas, S., Pandit, G.; Saradhi, I., et al., 2011. Long–range transport of soil dust and smoke pollution in the south asian region. Atmos. Pollut. Res. 2, 151–157.
7. Berdahl, P. and Fromberg, P. 1982. The thermal radiance of clear skies, Sol. Energy. 29: 299–314.
8. Bevis, M., Businger, S., Herring, T., Rocken, C., et al., 1992. GPS meteorology, Remote sensing of atmospheric water vapour using the Global Positioning System. Journal of Geophysical Research. 97: 15 784–15 801.
9. Brutsaert, W., 1975. On derivable formula for long-wave radiation from clear skies. Water Resour. Res., 11: 742-744.
10. CG1 handbook. CG1 pyrgeometer. Instruction manual. Kipp & Zonen. (2000). Delft. Holland.
11. Chantara, S., Sillapapiromsuk, S., Wiriya, W., 2012. Atmospheric pollutants in Chiang Mai (Thailand) over a five-year period (2005–2009), their possible sources and relation to air mass movement. Atmos. Environ. 60: 88–98.
12. Chen, X., Li, X., Yuan, X., Zeng, G., et al., 2018. Effects of human activities and climate change on the reduction of visibility in beijing over the past 36 years. Environ. Int. 116: 92–100.
13. Chou, M-D and Ridgway W., 1990. Infrared radiation parameterizations in numerical climate models. Journal of Climate. 4: 424-437.
14. Dilley, A. and O´Brien, D., 1998. Estimating downward clear sky long-wave irradiance at the surface from screen temperature and precipitable water, Q. J. R.Meteorol. Soc. 124: 1391-1401.
15. Dominick, D., Latif, M., Juahir, H., et al., 2012. An assessment of influence of meteorological factors on pm and 10 and no2 at selected stations in malasia. Sustain. Environ. Res. 22: 305–315.
16. Dufresne, J., Gautier, C., and Ricchiazzi, P., 2002. Long wave scattering effects of mineral aerosols, J. Atmos. Sci., 59: 1959 – 1966.

17. Dupont, J., Haeffelin, M., Drobinski, P., Besnard, T., 2008. Parametric model to estimate clear-sky longwave irradiance at the surface on the basis of vertical distribution of humidity and temperature, J. Geophys. Res.113, D07203.
18. Easter, R and Peters, L., 1994. Binary homogeneous nucleation: Temperature and relative humidity fluctuations, nonlinearity, and aspects of new particle production in the atmosphere, J. Appl. Meteorol., 33: 775–784.
19. Fernandes, F., Martins, E., Pedrosa, D., Evangelista. M., 2017. Relationship between climatic factors and air quality with tuberculosis in the federal district, brazil, 2003–2012. Braz. J. Infect. Dis. 21:369–375.
20. Garcıa, M., 2004. Simplified modelling of the nocturnal clear sky atmospheric radiation for environmental applications Ecological Modeling. 180: 395–406.
21. Gröbner J., Wacker, S., Vuilleumier, L., Kämpfer, N., 2009. Effective atmospheric boundary layer temperature from longwave radiation measurements, *J. Geophys. Res.,* 114, doi: 10.1 029/2009JD0 12274.
22. Harrison, R., Jones, A., Lawrence, R., 2004. Major component composition of PM10 and PM2.5 from roadside and urban background sites". Atmospheric Environment. 38: 4531-4538.
23. Haywood, J., Boucher, O. 2000. Estimates of the direct and indirect radiative forcing due to tropospheric aerosols A review. Review of Geophysics 38:513–543.
24. Holben B, Tanre D, Smirnov A, Eck T, Slutsker I., et al., (2001) An emerging ground-based aerosol climatology: aerosol optical depth from AERONET. J. Geophys. Res. 106:12067–12097. https://doi.org/10.1029/2001JD900014
25. Hueglin, C., Gehrig, R., Baltensperger, U., Gysel, M., Monn, C., and Vonmont, H.: Chemical characterization of PM2.5, PM10 and coarse particles at urban, near-city and rural sites in Switzerland, Atmos. Environ., 39, 637–651, 2005.
26. Idso SB, Jackson RD. Thermal radiation from the atmosphere. J Geophys. Res.1969; 74: 5397–5403.
27. Jayamurugan, R.; Kumaravel, B.; Palanivelraja, S.; Chockalingam, M.P. Influence of temperature, relative humidity and seasonal variability on ambient air quality in a coastal urban area. Int. J. Atmos. Sci. **2013**, 2013, 7.
28. Klingmüller K, Pozzer A , Metzger S , Georgiy L. Stenchikov , and Lelieveld J (2016) Aerosol optical depth trend over the Middle East. Atmos. Chem. Phys. 16: 5063–5073. https://doi.org/10.5194/acp-16-5063-2016
29. Kruk S, Vendrame F, Rocha R, Chou C, Cabral O (2010) Downward longwave radiation estimates for clear and all-sky conditions in the Sertãozinho region of São Paulo, Brazil. Theoretical and Applied Climatology. 99: 115-123.
30. Kutiel H, Furman H (2003) Dust storms in the Middle East: Sources of origin and their temporal characteristics. Indoor and Built Environment 12(6): 419-426.
31. Li, X.; Chen, X.; Yuan, X.; Zeng, G.; León, T.; Liang, J.; Chen, G.; Yuan, X. Characteristics of particulate pollution (PM2.5 and PM10) and their space scale dependent relationships with meteorological

elements in china. Sustainability **2017**, 9, 2330.

32. Liu C, Ou S (1990) Effects of tropospheric aerosols on the Solar radiative heating in a clear atmosphere. Journal of Theoretical and applied climatology 41: 97–106. https://doi.org/10.1007/BF00866432
33. Maghrabi A, Alotaib R (2017) Long-term variations of AOD from an AERONET station in the central Arabian Peninsula. Theoretical and Applied Climatology https://doi.org/10.1007/s00704-017-2328.
34. Maghrabi A, Al-Dosari A (2016) Effects on surface meteorological parameters and radiation levels of a heavy dust storm occurred in Central Arabian Peninsula. Atmospheric Research 182: 30-35.
35. Maghrabi A, Alharbi B, Tapper N (2011) Impact of the March 2009 dust event in Saudi Arabia on aerosol optical properties, meteorological parameters, sky temperature and emissivity. Atmospheric Environment 13 (45): 2164-2173.
36. Maghrabi A. H, 2012, Modification of the IR sky temperature under different atmospheric conditions in an arid region in central Saudi Arabia: Experimental and theoretical justification, Journal of Geophysical Research, VOL. 117, D19207.
37. Maghrabi A. H. and Alotaib R. N. Long-term variations of AOD from an AERONET station in the central Arabian Peninsula, 2017; Theoretical and Applied Climatology https://doi.org/10.1007/s00704-017-2328.
38. Maghrabi Abdullrahman, H.M. Al Dajani, Estimation of precipitable water vapor using vapor pressure and air temperature in an arid region in central Saudi Arabia, Journal of the Association of Arab Universities for Basic and Applied Sciences, Volume 14, Issue 1, 2013, Pages 1-8,
39. Maghrabi, A.H. and Clay, R.W, 2010, Precipitable water vapour estimation on the basis of sky temperatures measured by a single-pixel IR detector and screen temperatures under clear skies; Journal of meteorological Application; 17; 279-286.
40. Maghrabi, A.H. and Clay, R.W, 2011; Nocturnal Infrared Clear Sky Temperatures Correlated with Screen Temperatures and GPS-Derived PWV in Southern Australia. Energy and Conservation managements, 52, pp. 2925-2936.
41. Phairuang, W.; Hata, M.; Furuuchi, M. Influence of agricultural activities, forest fires and agro-industries on air quality in Thailand. J. Environ. Sci. **2017**, 52, 85–97.
42. Prata A J. A new long-wave formula for estimating downward clear-sky radiation at the surface, Quart. J. Roy. Meteor. Soc. 1996; 122: 1127-1151.
43. Querol X., A. Alastuey, S. Rodriguez, F. Plana, C. Ruiz, N. Cots, G. Massagué, O. Puig. “PM10 and PM2.5 source apportionment in the Barcelona Metropolitan area, Catalonia, Spain”. *Atmospheric Environment*. Vol. 35. 2001. pp. 6407-6419.
44. Ruckstuhl C, Philipona R, Morland J, Ohmura A. Observed relationship between surface specific humidity, integrated water vapor, and longwave downward radiation at different altitudes, J. Geophys. Res.2007; 112, D03302.
45. Smirnov A, Holben B, Dubovik O, Neil N, Eck T (2002) Atmospheric aerosol optical properties in the Persian Gulf. Atmospheric Science. 59: 620–634.

46. Streets, D.G., Yan, Fang, Chin, Mian, Diehl, Thomas, Mahowald, Natalie, Schultz, MartinW, Martin Wu, Ye, Y, Carolyne S (2009) Anthropogenic and natural contributions to regional trends in aerosol optical depth, 1980e2006. J. Geophys. Res. 114 (D00D18).
47. Svendsen H, Jensen HE, Jensen SE, Mogensen VO. The effect of clear sky radiation on crop surface temperature determined by thermal thermometry. Agric. For. Meteorol. 1990; 50: 239-243.
48. Swinbank W C. Long-wave radiation from clear skies, *Quart. J. Roy, Meteor. Soc. 1963;* 89:339–48.
49. Tian, G.; Qiao, Z.; Xu, X. Characteristics of particulate matter (PM10) and its relationship with meteorological factors during 2001–2012 in beijing. Environ. Pollut **2014**, 192, 266–274.
50. Vardoulakis S., P. Kassomenos. 2008. Sources and factors affecting PM10 levels in two European cities: Implications for local air quality management". *Atmospheric Environment*. Vol. 42.. pp. 3949-3963.
51. Viudez-Mora, A., J. Call J. A. Gonzalez, and M. A. Jimenez (2009), Modeling atmospheric longwave radiation at the surface under cloudless skies, *J. Geophys. Res.,* 114, D18107.
52. Wang, J.; Ogawa, S. Effects of meteorological conditions on PM2.5 concentrations in Nagasaki, Japan. Int. J. Environ. Res. Public Health **2015**, 12, 9089–9101.
53. Wild M, Ohmura A, Gilgen H, Morcrette J, Slingo A (2001). Evaluation of Downward Radiation in General Circulation Models. Journal of Climate. 14: 3227-3229.
54. Xia X, Li Z, Wang P, Chen H, Cribb M (2007) Estimation of aerosol effects on surface irradiance based on measurements and radiative transfer model simulations in northern China, J. Geophys. Res.112, D22S10, doi:10.1029/2006JD008337

Tables

Table (1) presents the mean, standard deviation, and the minimum and maximum values of the hourly mean values of the variables considered between March 2015 and September 2019. The aerosol optical depth data were recorded between March 2014 to August 2015.

	PM_{10} ($\mu g/m^3$)	$PM_{2.5}$ ($\mu g/m^3$)	PWV (mm)	T (°C)	Wind Speed (m/s)	LW (Wm^2)	AOD N=1468
Mean	141.67	39.9	19.02	29.21	1.89	383.99	0.40
Standard Deviation	71.90	34	4.35	9.34	1.50	69.75	0.25
Minimum	8.00	1.00	6.35	3.41	0.00	238.55	0.03
Maximum	442	439.00	38.50	46.22	5.49	505.29	2.05

Table 2: Presents the regression equations and the statistical indicators (correlation coefficient (R), root mean square error (RMSE), between the daily mean values of the downward LW radiation data and the air temperature (T), precipitable water vapor (PWV), particulate matter concentrations PM_{10} and $PM_{2.5}$, wind speed (WS) and aerosol optical depth (AOD) between 2014 and 2019. The AOD data is from 2014 to August 2015.

Category	Regression Equation	RMSE W/m^2	R
PM_{10}		39.29	0.32
$PM_{2.5}$		38.42	0.32
T		8.05	0.98
PWV		37.71	0.36
WS		41.43	0.01
AOD n=195		34.73	0.69

Figures

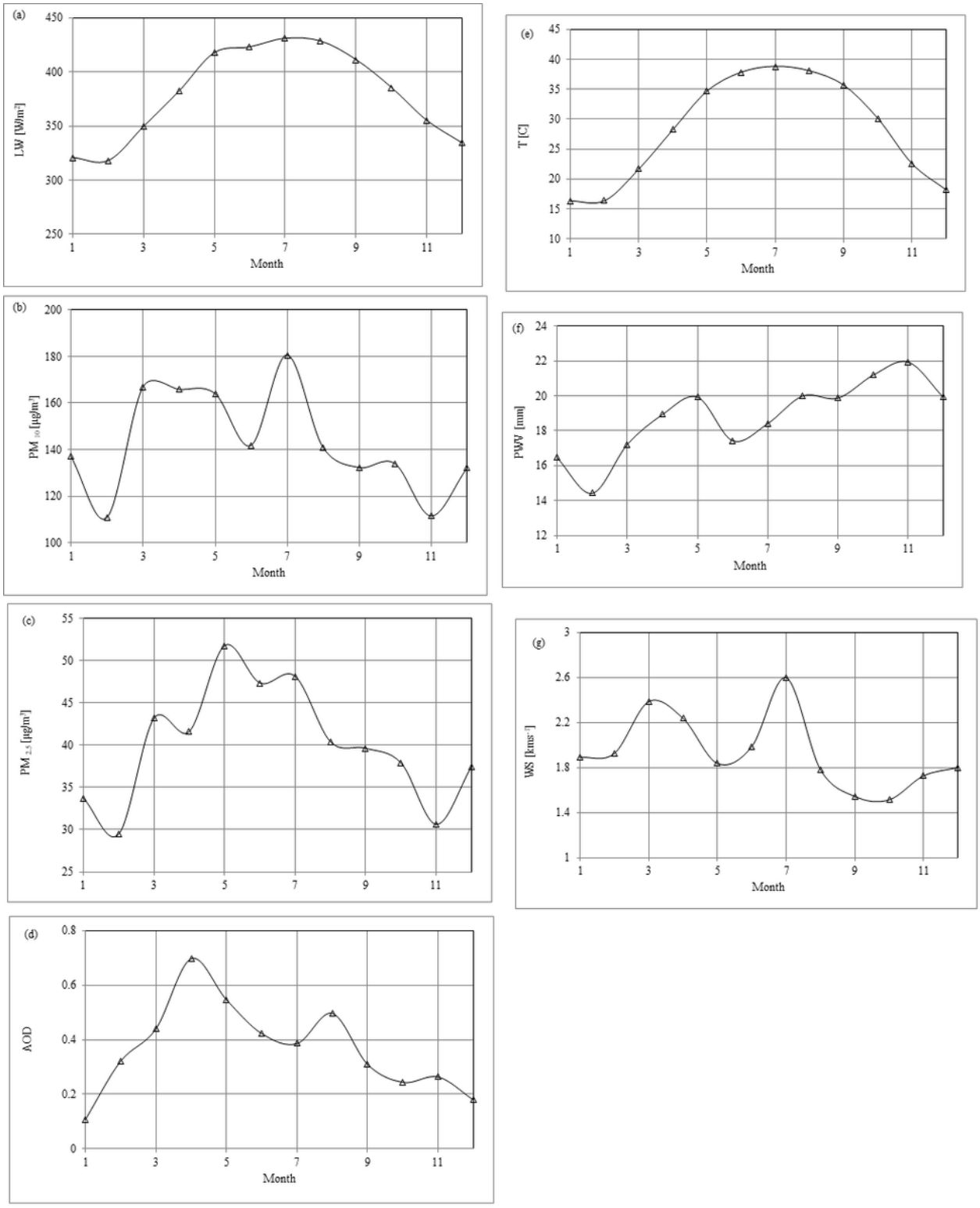

Figure 1

shows the monthly variations of the (a) LW radiation, (b) PM10 , (c) PM2.5, (d) AOD, (e) air temperature (f) PWV, and (g) the wind speed during the study period.

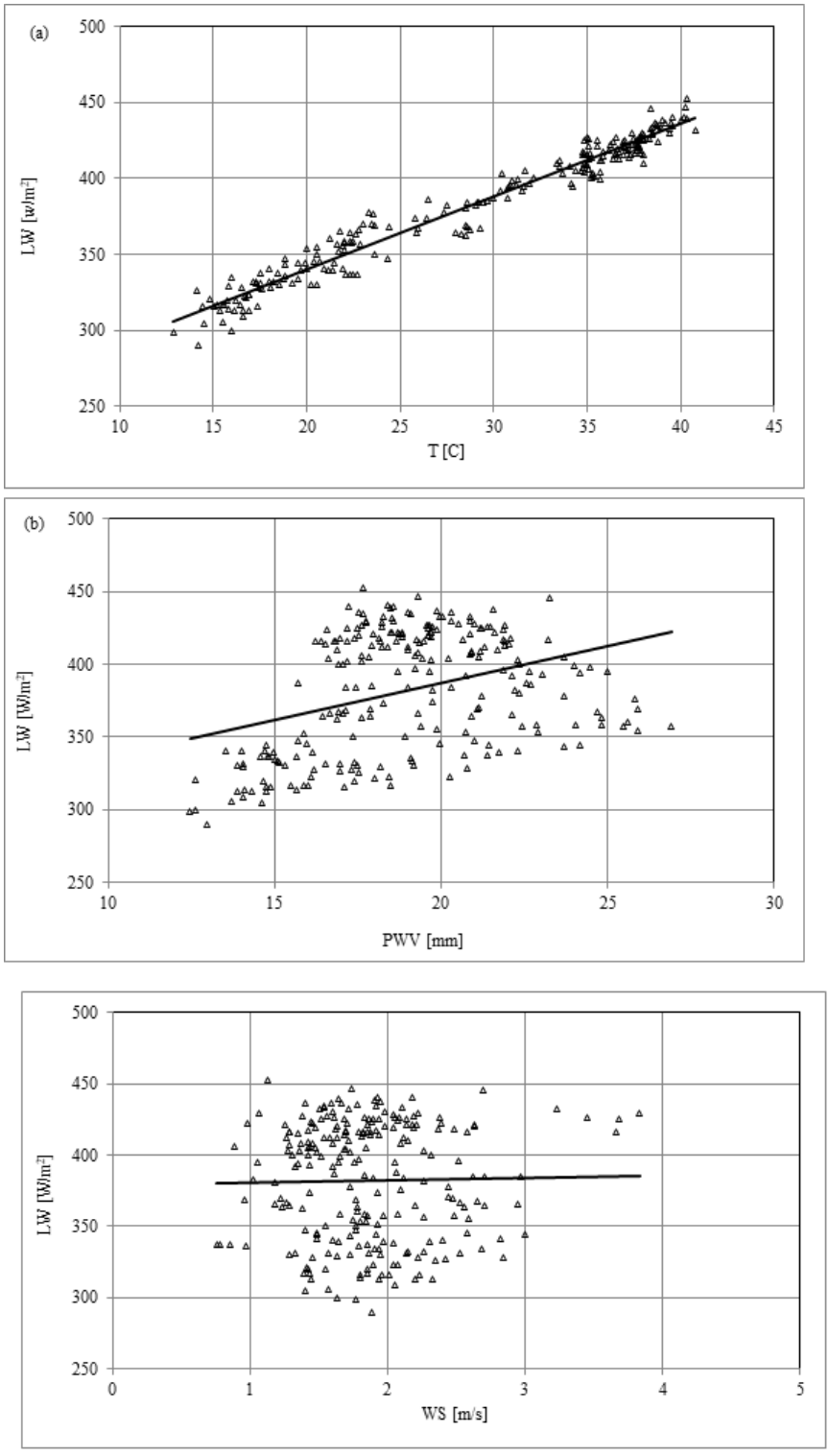

Figure 2

Scatter plot between the daily mean measured downward LW radiation data and (a) air temperature, (b) the precipitable water vapor (PWV), and wind speed (WS) between 2014 and 2019. The thick lines represent the regression lines.

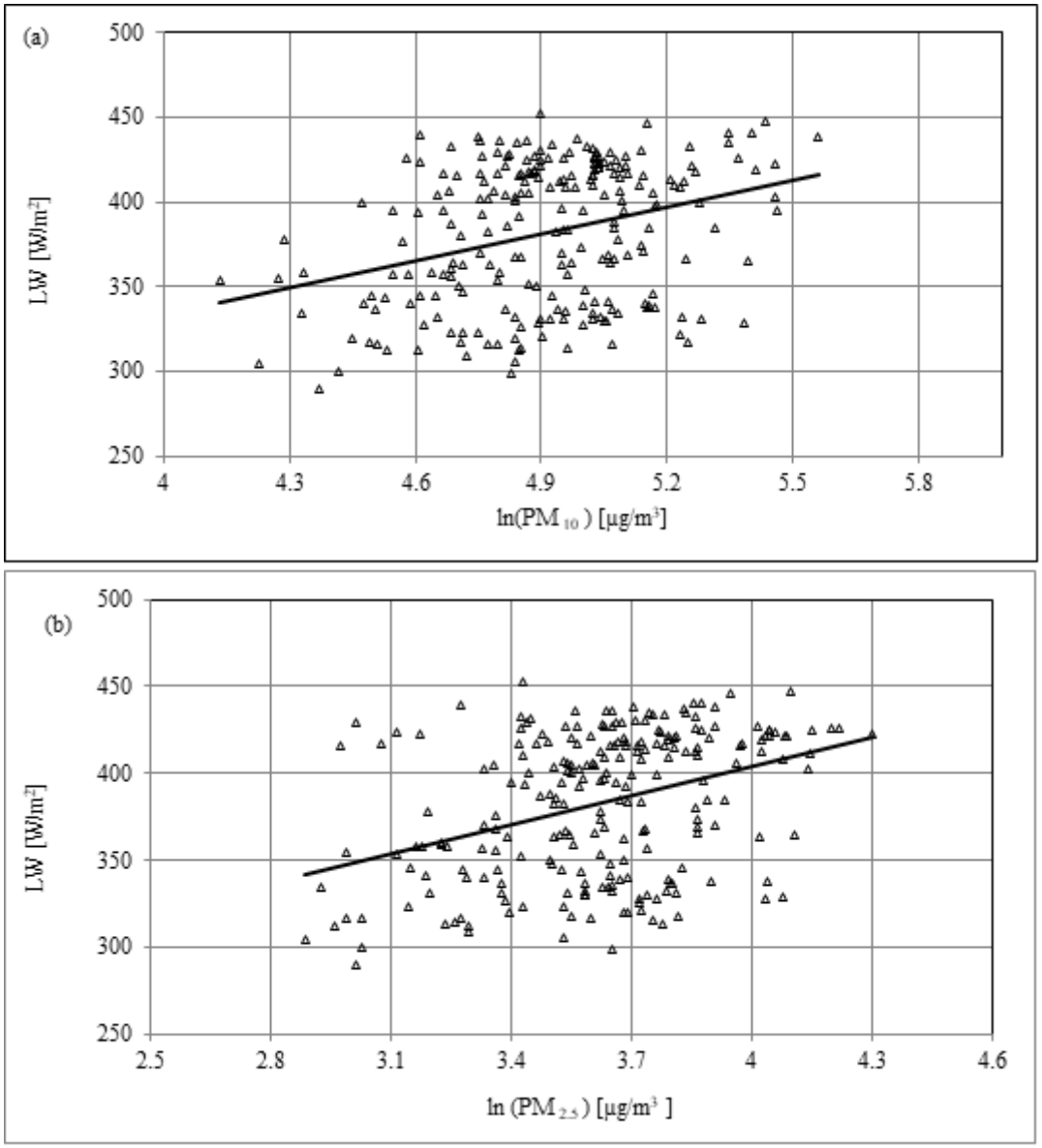

Figure 3

Scatter plot between the daily mean measured downward LW radiation data and (a) PM10 and PM2.5 during the period 2014–2019. The thick lines are the regression lines.

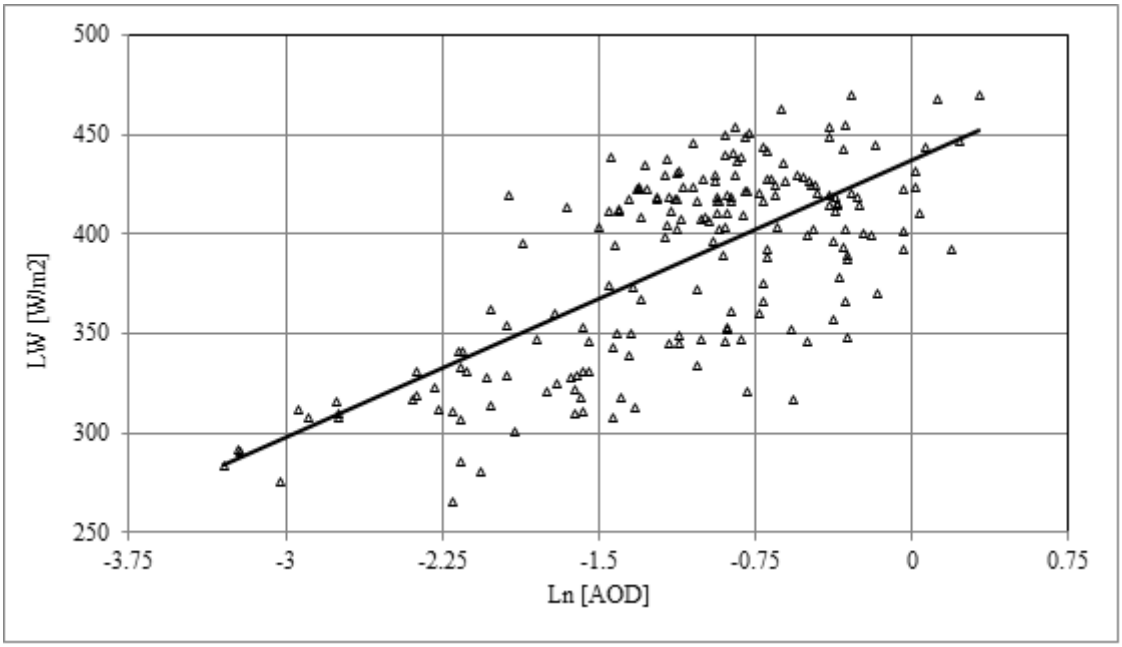

Figure 4

A scatter plot between the daily measured downward LW radiation data and the AOD at 500 microns between 2014 and 2015. The thick lines are the regression lines.

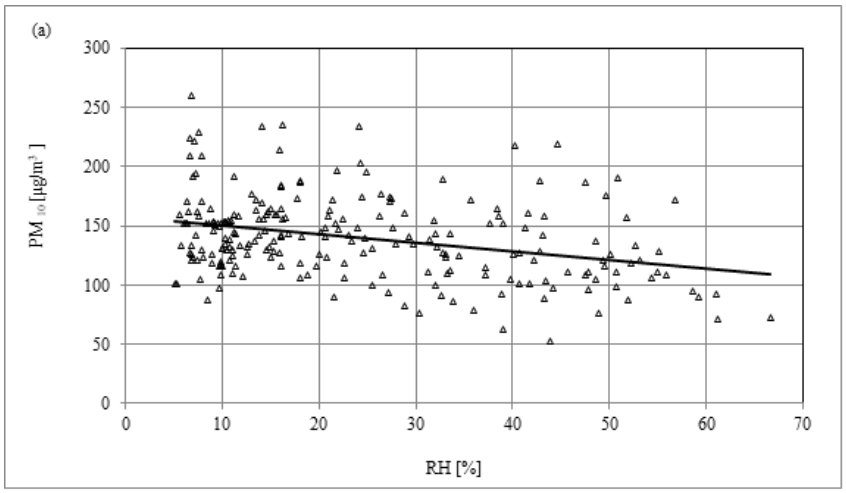

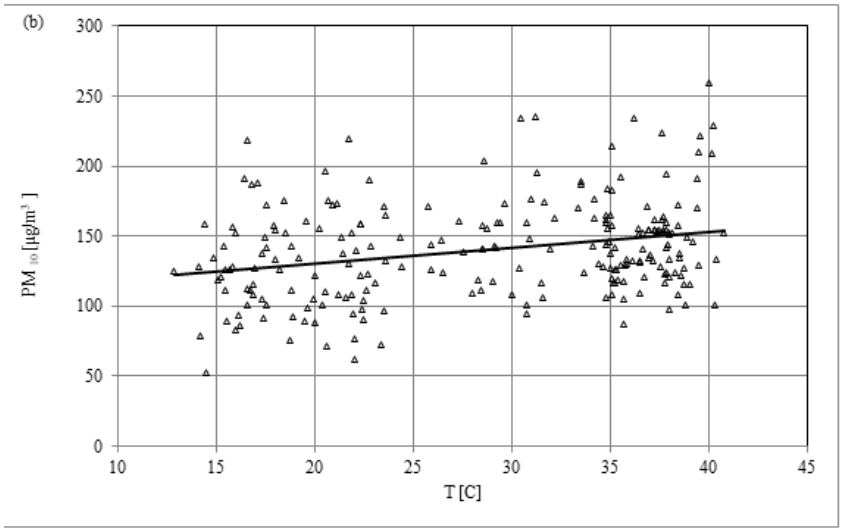

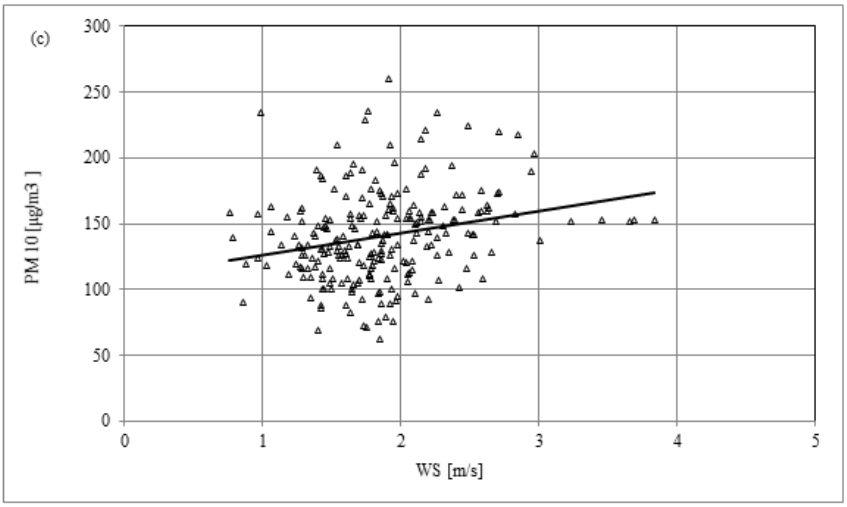

Figure 5

Scatter plot between the daily mean measured downward LW radiation data and (a) relative humidity (RH), (b) air temperature (T), and wind speed (WS) between 2014 and 2019. The thick lines represent the regression lines.